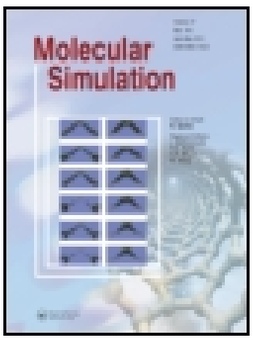

Molecular Simulation

ISSN: (Print) (Online) Journal homepage: https://www.tandfonline.com/loi/gmos20

A computational analysis of the binding free energies of apoptosis signal-regulating kinase 1 inhibitors from different chemotypes

Galyna P. Volynets, Larysa V. Pletnova, Vladislav M. Sapelkin, Oleksandr V. Savytskyi & Sergiy M. Yarmoluk

To cite this article: Galyna P. Volynets, Larysa V. Pletnova, Vladislav M. Sapelkin, Oleksandr V. Savytskyi & Sergiy M. Yarmoluk (2021): A computational analysis of the binding free energies of apoptosis signal-regulating kinase 1 inhibitors from different chemotypes, Molecular Simulation, DOI: 10.1080/08927022.2021.1922686

To link to this article: https://doi.org/10.1080/08927022.2021.1922686

MOLECULAR SIMULATION
https://doi.org/10.1080/08927022.2021.1922686

Taylor & Francis
Taylor & Francis Group

A computational analysis of the binding free energies of apoptosis signal-regulating kinase 1 inhibitors from different chemotypes

Galyna P. Volynets [a,b], Larysa V. Pletnova[a], Vladislav M. Sapelkin[a], Oleksandr V. Savytskyi[c] and Sergiy M. Yarmoluk[a]

[a]Department of Medicinal Chemistry, Institute of Molecular Biology and Genetics, NAS of Ukraine, Kyiv, Ukraine; [b]Scientific Services Company Otava Ltd., Kyiv, Ukraine; [c]Department of Protein Engineering and Bioinformatics, Institute of Molecular Biology and Genetics, NAS of Ukraine, Kyiv, Ukraine

ABSTRACT

Apoptosis signal-regulating kinase 1 (ASK1) has recently emerged as an attractive molecular target for pharmaceutical intervention. Several classes of small-molecular ASK1 inhibitors have been identified. In this article, we analysed the binding of small-molecular inhibitors from different chemotypes with ASK1 using molecular dynamic simulations. The umbrella sampling technique was used to calculate the binding free energy (ΔG) for these compounds with ASK1 ATP-binding pocket. According to the obtained results, umbrella sampling gave correct ranking of the binding affinities for investigated inhibitors relative to their experimental pIC_{50} values and can be useful for further structure-based design of ASK1 inhibitors to accelerate lead optimisation.

Trial registration: ClinicalTrials.gov identifier: NCT02466516..

ARTICLE HISTORY
Received 18 November 2020
Accepted 19 April 2021

KEYWORDS
Apoptosis signal-regulating kinase 1; ASK1; inhibitor; umbrella sampling; binding free energy

1. Introduction

Apoptosis signal-regulating kinase 1 (ASK1) is a ubiquitously expressed Ser/Thr protein kinase which is activated in response to various stimuli such as reactive oxygen species [1], endoplasmic reticulum stress [2], lipopolysaccharide [3], tumour necrosis factor α (TNF-α) [4]. ASK1 has been reported to be involved in a number of neurodegenerative [5–7], cardiovascular [8], autoimmune diseases [9,10], diabetes [11], cancer [12,13], etc. Consequently, ASK1 inhibitors may have the potential to treat clinically important human pathologies [14,15]. There are several classes of small-molecular ASK1 inhibitors have been already published [9,14,16–25]. It should be noted that one of the ASK1 inhibitors, GS-4997, discovered by Gilead Sciences is now undergoing clinical trials (https://clinicaltrials.gov/ct2/show/NCT02466516) which supports the notion that ASK1 is considered as a 'druggable' molecular target. According to the literature data, the main approach for the development of ASK1 inhibitors at present time is a structure-based design. For example, recently, starting from purine, pyrimidine and quinazoline scaffolds, using a structure-based drug design, a series of ASK1 inhibitors among the derivatives of 2-arylquinazoline has been identified [26]. Using deconstruction and re-optimisation of known ASK1 inhibitors, novel efficient ASK1 inhibitors have been developed [27–32].

The thermodynamic characterisation of protein–ligand interaction is useful for compound activity optimisation during the structure-based drug design. One of the latest experimental techniques for characterising protein–ligand binding affinity is isothermal titration calorimetry (ITC). Due to some concerns of this method, such as large sample requirement, limitation to the determination of the binding constant (this method cannot measure too strong ($Ka > 10^9$ M^{-1}) or too weak binding ($Ka < 10^3$ M^{-1})), high sensitivity to the presence of chemical reagents such as TRIS, DTT, DMSO, etc. in solution, computational approaches can be useful to obtain thermodynamic characteristics of ligand binding. Earlier, correlations of experimental ITC measurements with umbrella sampling calculations have been identified for Proviral integration site for Moloney murine leukaemia virus-1 (PIM-1) protein kinase [33]. Moreover, there are a number of recent published works demonstrating that the umbrella sampling algorithm allows calculate free energy of ligand binding to the receptor, which is either close to experimental or significantly correlates with experimental values [34–37].

In order to establish whether the umbrella sampling algorithm can be useful for structure-based optimisation of ASK1 inhibitors, we have calculated binding free energy for the compounds from different chemical chemotypes with ASK1 ATP-binding pocket which were identified during multikinase profiling of a set of fragment-sized compounds [38] and one of them was identified as a close analogue of known ASK1 inhibitor [18].

2. Methods

2.1. Molecular dynamics

All molecular dynamic (MD) simulations were carried out with GROMACS v.4.5 [39–41]. The starting coordinates used for all simulations were from the crystal structures of ligands bound to the ASK1 with PDB accession codes: 4BF2, 4BHN, 4BID, 4BIE and 4BIB [18]. GROMOS96 force field was used for MD experiments [42]. Energy minimisation of

CONTACT Galyna P. Volynets g.p.volynets@gmail.com
Supplemental data for this article can be accessed at https://doi.org/10.1080/08927022.2021.1922686

ligand–receptor complexes was performed in explicit water environment with steepest descent energy minimisation algorithm for 1000 relaxation steps. The minimised structure was taken for position restrain dynamics using the relaxation time 20 ps. Then, MD simulation during 20 ns was carried out. The integration of the equations of motion was performed using the leap-frog algorithm [43] and canonical (NVT) ensemble. For electrostatics treatment, Particle Mesh Ewald algorithm was applied [44,45].

2.2. Free energy calculation by umbrella sampling

The umbrella sampling algorithm and the Weighted Histogram Analysis Method (WHAM) [46] were used to calculate the free energy profile for the separation of five ASK1-inhibitor complexes. The starting coordinates used for umbrella sampling simulations were from the crystal structures with PDB accession codes: 4BF2, 4BHN, 4BID, 4BIE and 4BIB [18].

Topology files for ligands were generated using Dundee PRODRG server (accessed 20 January 2017) [47]. We used ligand GRO files containing polar/aromatic H's. Topology file for protein kinase ASK1 has been generated from PDB-file using pdb2gmx command. The system was set up using the Gromos96 53a6 force field [42] and solvated with the SPC water model [48]. In the case of PDB-structure 4BIB, several atom types were missed in Gromos96 53a6 force field, thus Charmm27 force field [49] and TIP3P water model [50] were used.

The centre of mass of the ASK1-inhibitor complex has been placed at (4.0, 4.0, 4.0 nm) in a box of dimensions $12 \times 12 \times 12$ nm using editconf command. Then, the system was solvated with genbox command and neutralised using Na^+ or Cl^- ions according to the charge of the system using genion command.

The number of atoms for five ASK1:inhibitor:water:ion systems used for umbrella sampling simulations was as follows: 4BF2: 2708:46:68902:5; 4BIB: 4229:37:68917:5; 4BID: 2740:47:68951:4; 4BIE: 2747:30:68896:4; 4BHN:2765:48:68918:6.

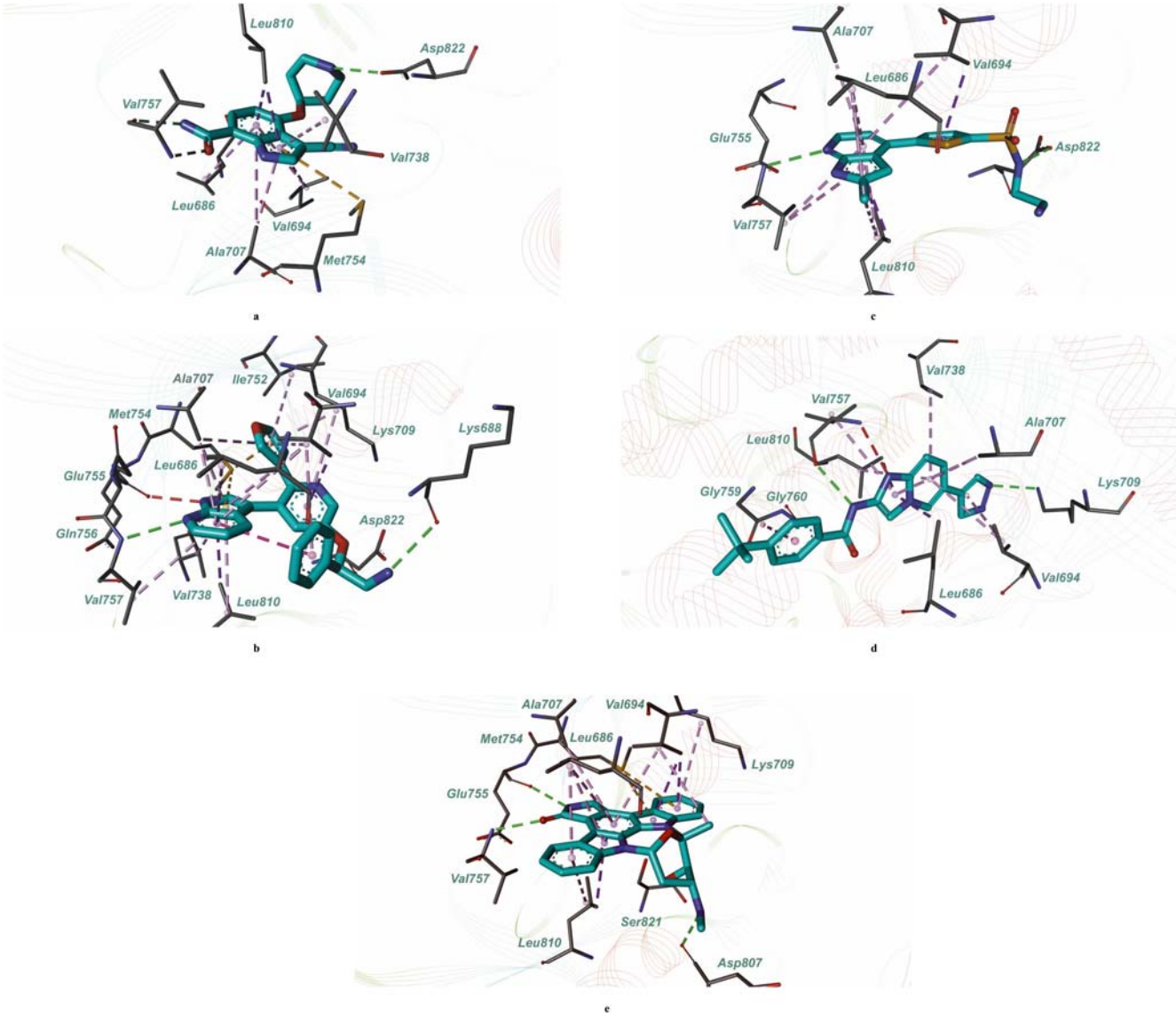

Figure 1. (Colour Online) The binding modes of compounds **1** (a), **2** (b), **3** (c), **4** (d) and staurosporine (e) in the active site of the ASK1 catalytic subunit. Hydrogen bonds are shown by the green dotted lines and hydrophobic interactions are presented by magenta dotted lines.

The periodic boundary conditions and the particle mesh Ewald method [44,45] were used with a nonbonded cut-off of 9 Å. Each system was first energy minimised using 5000 steps of steepest descent method followed by NPT equilibration for 100 ps (50,000 steps). For NPT equilibration we used Berendsen thermostat with temperature = 310 K and Parrinello-Rahman barostat with pressure = 1 bar. Using make_ndx command we have defined custom index group for pulling simulation. Pulling of ligands for each system has been performed in Y-dimension using a spring constant of 1000 kJ/(mol nm^2) and pulling rate 0.01 nm/ps, as described earlier [51]. A series of configurations along Y-axis has been generated corresponding to each of the frames saved in the continuous pulling simulation. To measure the distance between protein and ligand on all of these frames, we have used Perl script to iteratively call g_dist command. The total path with a length of 4.5 nm was divided into 0.1 nm wide equidistant windows. We used final centre of-mass (COM) distance between protein kinase ASK1 and small-molecular inhibitor of 4.5 nm since the plot of PMF vs. distance reached a plateau for all investigated systems and applied window spacing 0.1 nm which allowed for increasing detail at smaller COM distance, and resulted in about 20 windows. Each coordinate file, which is required to obtain 0.1-nm spacing, has been prepared for umbrella sampling simulations. At first, NPT equilibration in each window was performed during

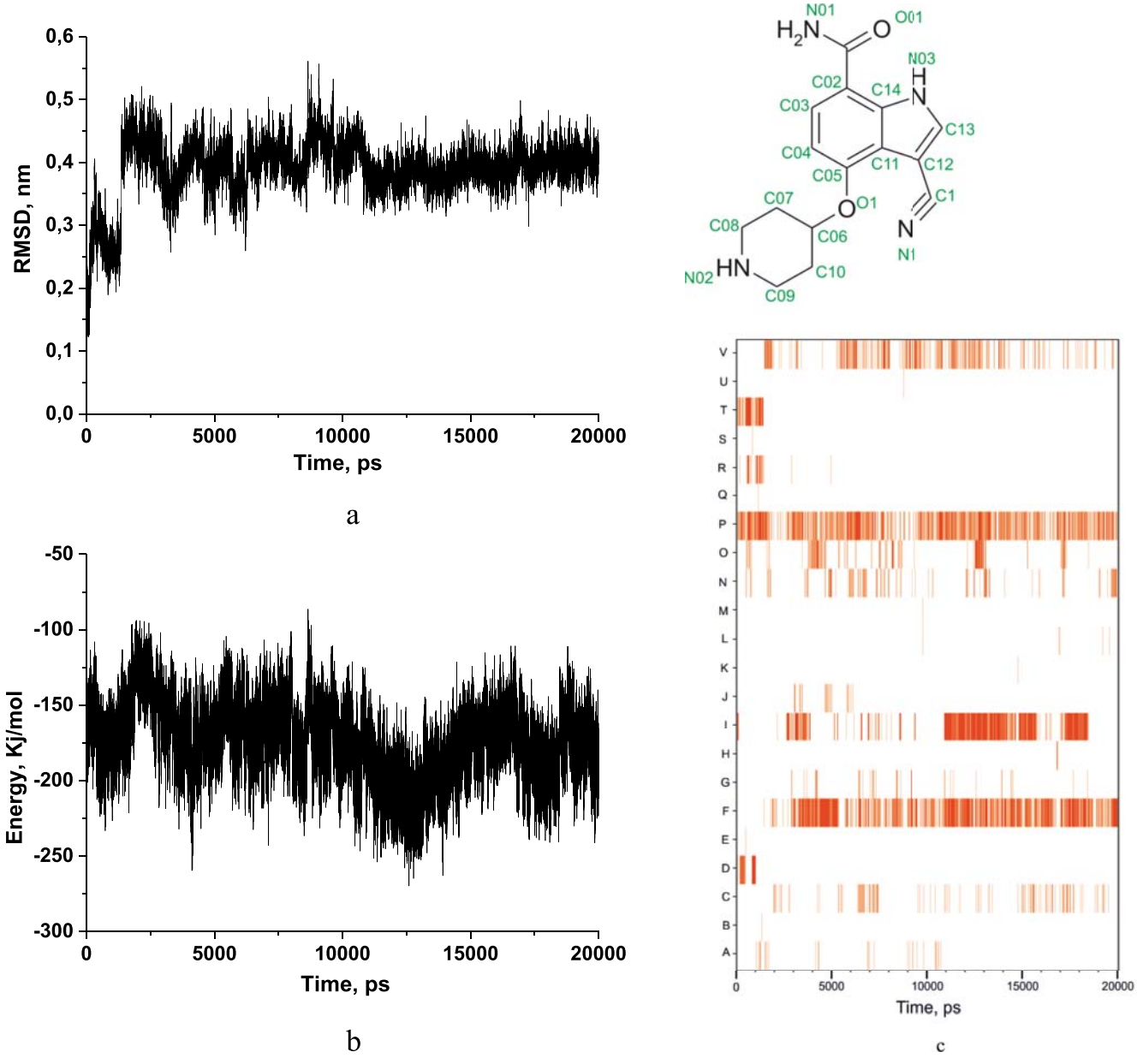

Figure 2. (Colour Online) Molecular dynamic (MD) results of compound **1** in complex with ASK1 during 20-ns MD simulation: RMSD of compound **1** (a), sum of Coulomb and Lennard-Jones interaction energies for compound **1**-ASK1 complex (b), hydrogen-bond existence map of compound **1**-ASK1 complex (c).

500 ps (250,000 steps). Then, each input file was passed to umbrella sampling simulation. Then, using WHAM we have extracted the potential of mean force (PMF), which yields the ΔG for the binding/unbinding process.

The file with a list of commands and MDP files used during umbrella sampling simulations for ASK1-inhibitor complexes (PDB ID: 4BIC and 4BIB) is available as Supplementary material.

3. Results and discussion

In this work, we have used the umbrella sampling algorithm to determine the PMF for apoptosis signal-regulating kinase 1 (ASK1) with five compounds belonging to four different chemotypes – indole-carboxamides (compound **1**), 7-azaindoles (compound **2** and compound **3**), imidazopyridines (compound **4**) and indolocarbazole (staurosporine).

The complexes of these compounds with amino acid residues in the ATP-binding site of ASK1 are presented in Figure 1.

In order to establish that the complexes are stable, we have performed MD simulation for each complex during 20 ns. As it can be seen from the RMSD plots, all investigated complexes are stable without tendencies to dissociation (Figures 2–6(a)).

It is turned out that the compound **1** forms hydrogen bonds with Val757, Ser761, Ser821, Asp822, Leu686 and Gly759 during almost all the times of MD simulation (Figure 2(c)). Some disposition of the ligand in the ATP-binding pocket is observed at 1 ns of MD simulation which can be caused by the disruption of hydrogen bonds with Gly759 and carbonyl group of Val757 which leads to the slight increase of the energy (Figure 2(b)).

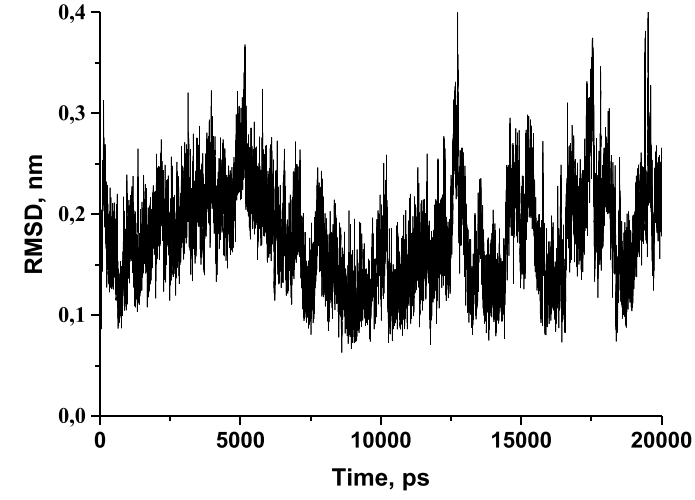

a

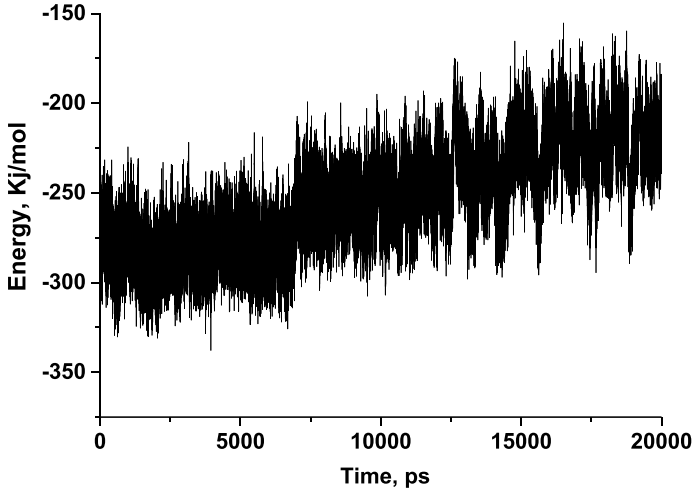

b

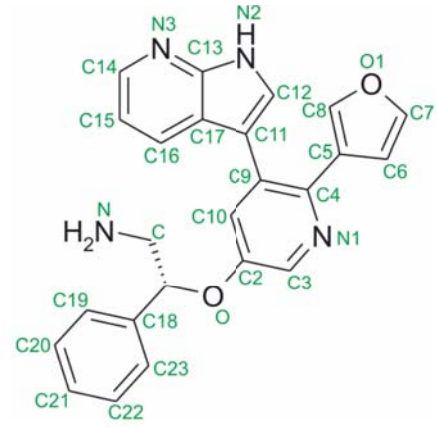

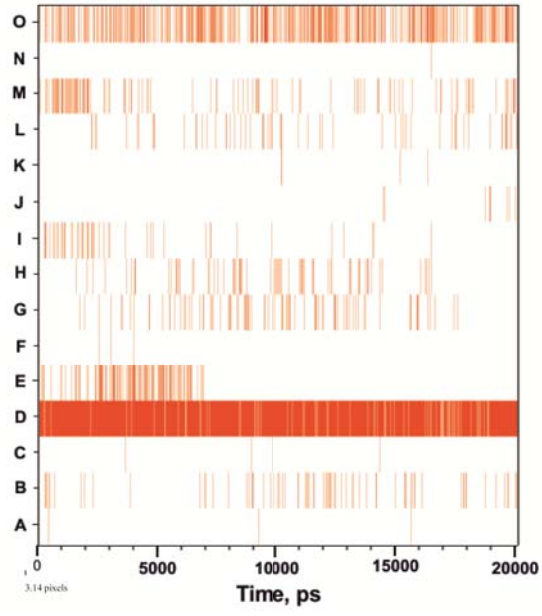

c

Figure 3. (Colour Online) Molecular dynamic (MD) results of compound **2** in complex with ASK1 during 20-ns MD simulation: RMSD of compound **2** (a), sum of Coulomb and Lennard-Jones interaction energies for compound **2**-ASK1 complex (b), hydrogen-bond existence map of compound **2**-ASK1 complex (c).

The stabilisation of the compound **2**-ASK1 complex obviously is supported by the formation of hydrogen bonds with Lys709, Val757, Asp807, Asp822 and Glu755 during almost all the times of MD (Figure 3(c)). The increase of the energy is observed after 7 ns of simulation (Figure 3(b)) which can be explained by the disruption of hydrogen bond with Lys688 (Figure 3(c)).

As it can be seen from Figure 4, some disposition of compound **3** in the ATP-binding pocket is observed at 9 ns of MD simulation. The presented hydrogen bond network correlates well with the energy of the complex. The decrease of the energy of the complex, which reflects further stabilisation (Figure 4(b)), can be associated with the disruption of hydrogen bonds of the ligand with amino acid residues Lys688, Val757, Asp807, Asn808 and by the formation of hydrogen bonds with amino acid residues Thr690, Asp803 and Thr825 (Figure 4(c)).

Apparently, the stabilisation of the complex compound **4**-ASK1 is due to the formation of the hydrogen bonds with Lys709, Val757 and Asp822 during all the times of MD simu-

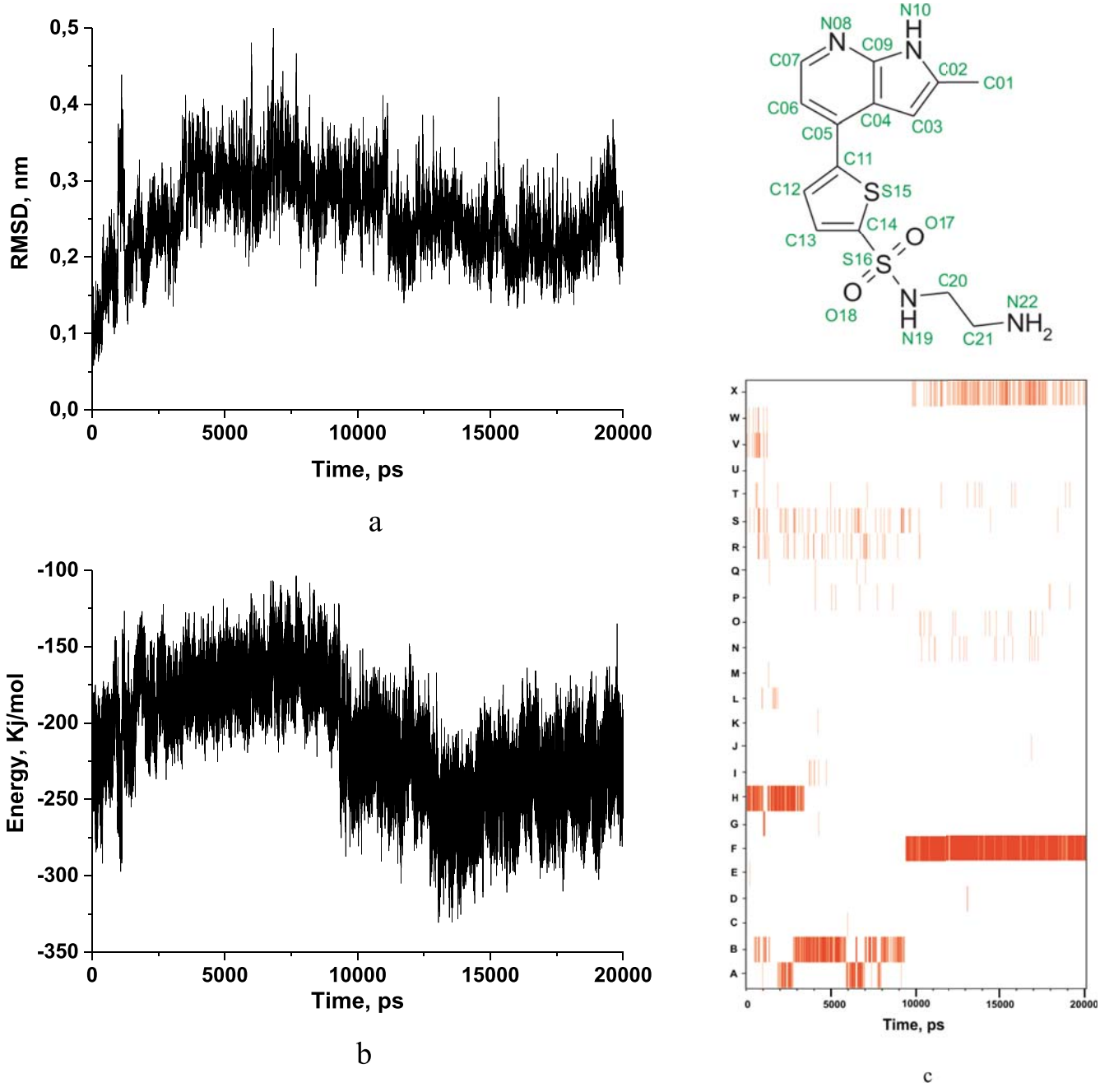

Figure 4. (Colour Online) Molecular dynamic (MD) results of compound **3** in complex with ASK1 during 20-ns MD simulation: RMSD of compound **3** (a), sum of Coulomb and Lennard-Jones interaction energies for compound **3**-ASK1 complex (b), hydrogen-bond existence map of compound **3**-ASK1 complex (c).

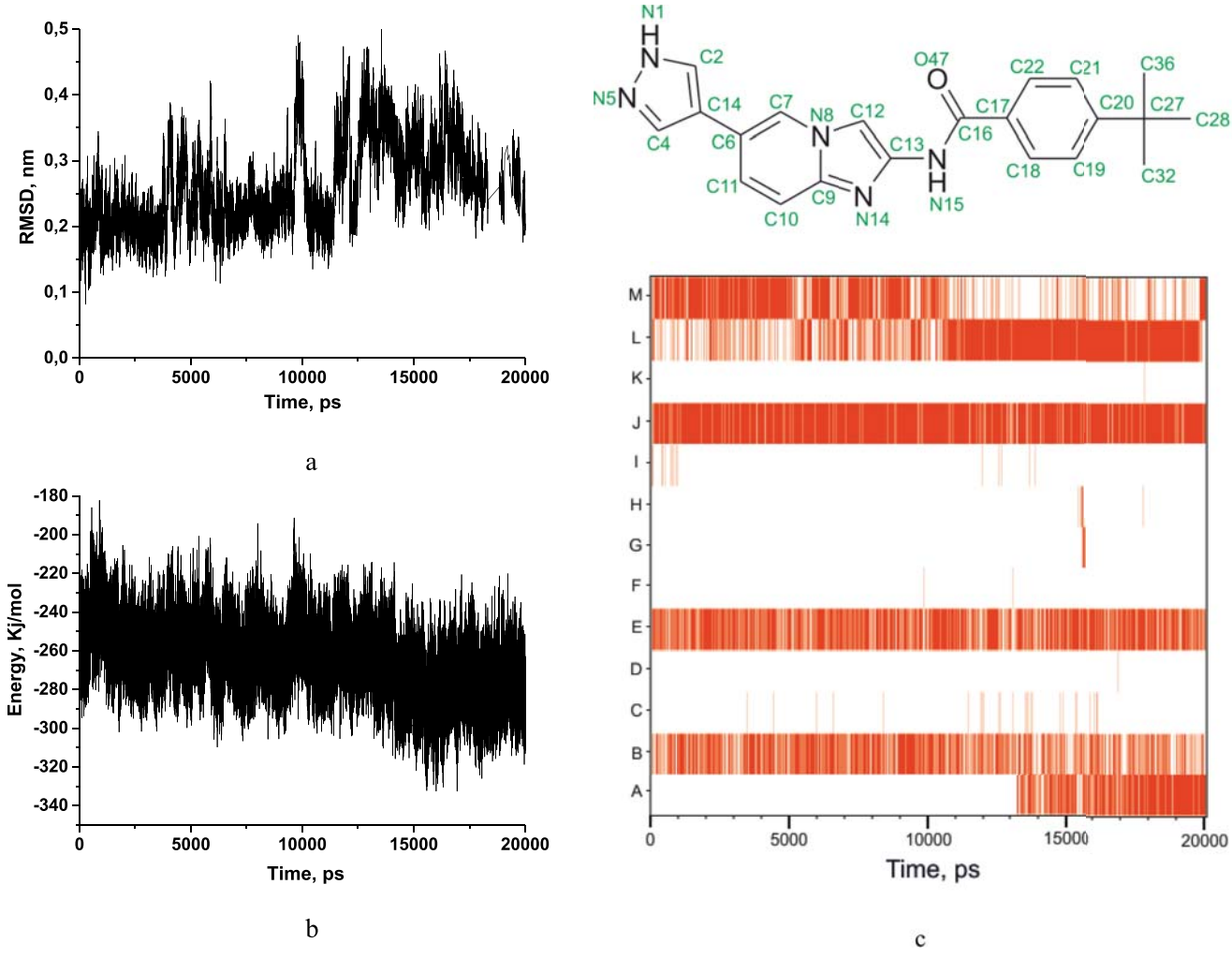

Figure 5. (Colour Online) Molecular dynamic (MD) results of compound **4** in complex with ASK1 during 20-ns MD simulation: RMSD of compound **4** (a), sum of Coulomb and Lennard-Jones interaction energies for compound **4**-ASK1 complex (b), hydrogen-bond existence map of compound **4**-ASK1 complex (c).

lation (Figure 5(c)). The formation of additional hydrogen bond with Gly687 possibly leads to a slight decrease of the energy which means stronger complex stabilisation (Figure 5(b)).

As shown in Figure 6, staurosporine is displaced in the ATP-binding pocket of ASK1 at 3 ns of MD simulation which leads to the increase of the energy. This disposition can be caused by the loss of hydrogen bonds with amino acid residues in the hinge region such as Val757 and Glu755. The decrease of energy is observed at 12 ns which can be associated with the formation of hydrogen bonds with Asp807 and Asp822. Then, the disruption of these hydrogen bonds possibly leads again to the increase of the energy.

The umbrella sampling algorithm was used to calculate binding free energy (ΔG) for these compounds with ASK1 ATP-binding pocket. Pulling of the ligands was performed in the Y-dimension in order to allow ligand move from active site into water (Figure 7).

Δ*G*b has been determined from PMF plots as the difference between the PMF with the ligand bound minus the ligand when it is unbound (Figure 8).

As can be seen from Table 1, the most active compounds **2** and **4** with experimental pIC_{50} values of 7.9 ± 0.1 have the lowest values of binding free energy (−21 and −22 kcal/mol, respectively), which means that these compounds bind with enzyme with higher affinity and vice versa, the compounds **1** and **3** with experimental pIC_{50} values of 6.1–6.2 have higher values of binding free energy (−16 and −14.5 kcal/mol, respectively), which means that these compounds bind with enzyme with lower affinity. It should be noted that according to MD simulation the compounds **2** and **4** also have lower values of the sum of Coulomb and Lennard–Jones interaction energies and have more stable hydrogen bond networks than the compounds **1**, **3** and staurosporine.

Possibly, different binding modes of compounds in the ATP-binding site of protein kinase ASK1 can reflect different shapes of the PMF profiles.

Since the obtained calculated results of binding free energy values are in a good agreement with the trends observed for experimental pIC_{50} values (binding data), the umbrella sampling algorithm can be considered as a quite acceptable approach for structure-based inhibitor optimisation.

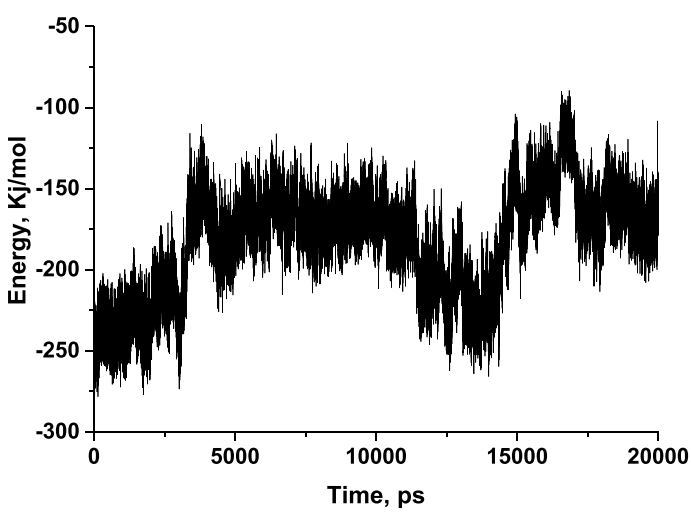

a

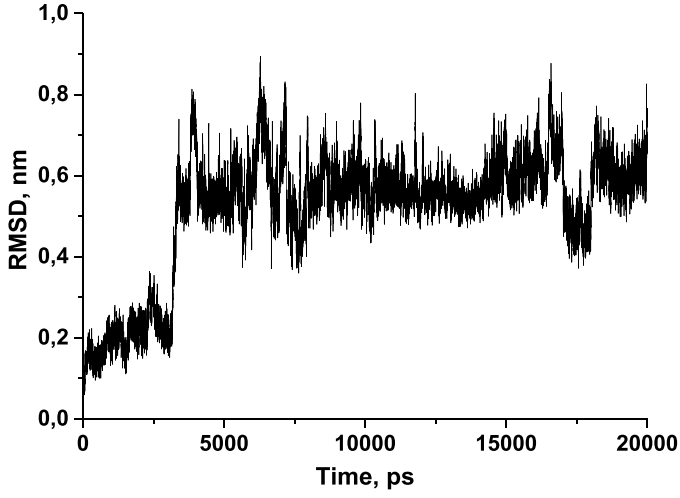

b

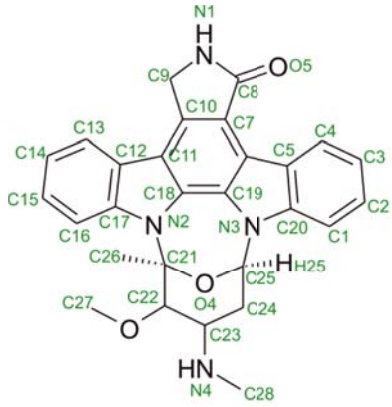

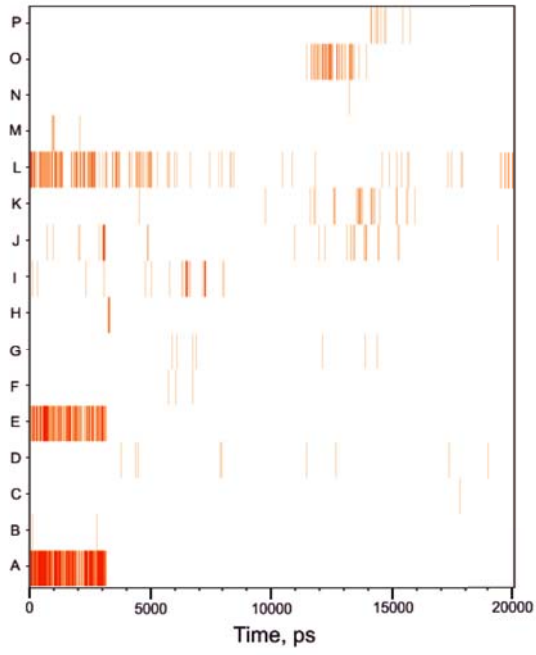

c

Figure 6. (Colour Online) Molecular dynamic (MD) results of staurosporine in complex with ASK1 during 20-ns MD simulation: RMSD of staurosporine (a), sum of Coulomb and Lennard-Jones interaction energies for staurosporine-ASK1 complex (b), hydrogen-bond existence map of staurosporine-ASK1 complex (c).

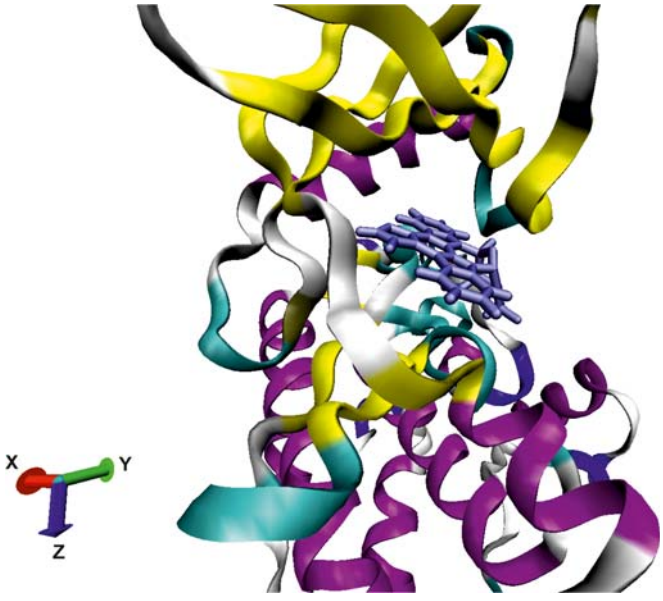

Figure 7. (Colour Online) Molecular rendering of the ASK1-ligand system indicating axes X, Y, Z.

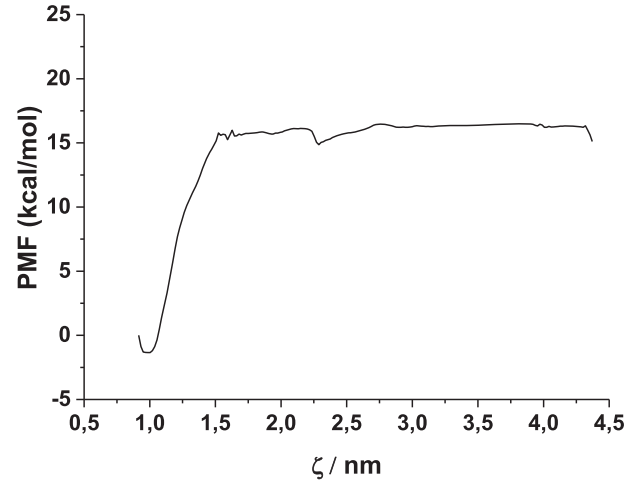

a

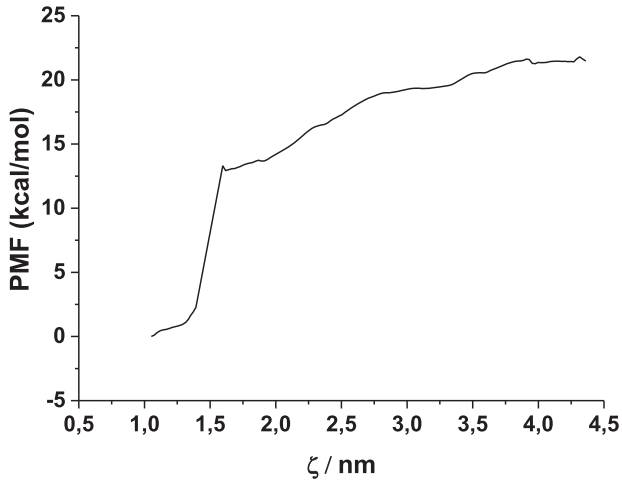

d

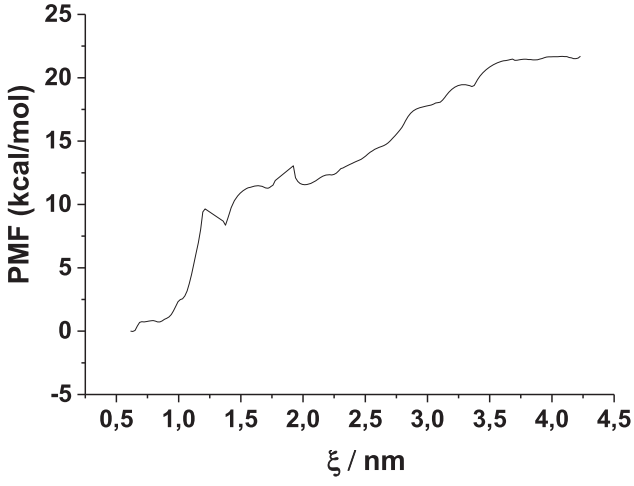

b

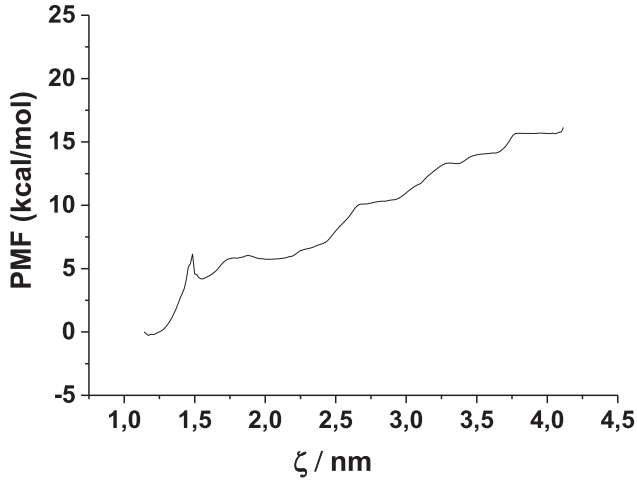

e

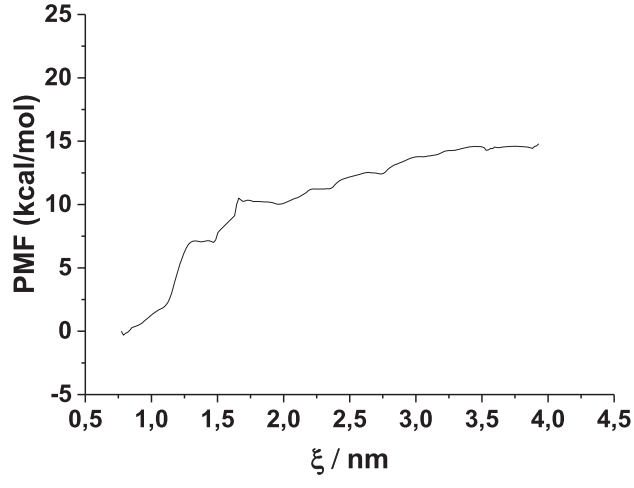

c

Figure 8. Potential of Mean Force (PMF) for unbinding of the complexes of protein kinase ASK1 with compound **1** (a), **2** (b), **3** (c), **4** (d) and staurosporine (e).

Table 1. Compound structures and their experimental pIC_{50} values towards protein kinase ASK1 and calculated PMF values for ASK1-ligand unbinding (see Figure 8).

Compound	Structure	pIC_{50}	PMF, kcal/mol
Compound 1	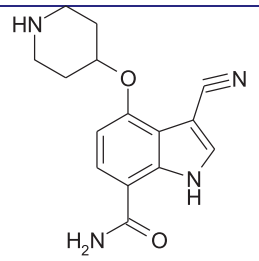	6.2 ± 0.5	−16
Compound 2	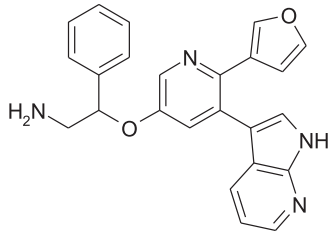	7.9 ± 0.1	−21
Compound 3	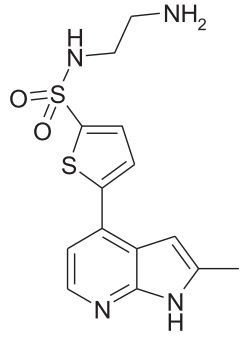	6.1 ± 0.1	−14.5
Compound 4	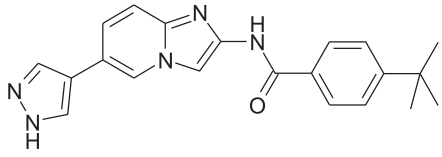	7.9 ± 0.1	−22
Staurosporine	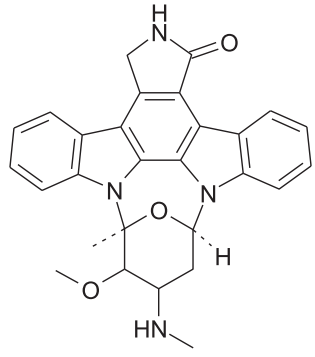		−16

Disclosure statement

No potential conflict of interest was reported by the author(s).

Funding

This work was supported by the Grant of the State Fund for Fundamental Researches (SFFR F63) in Ukraine [grant number 0116U006538] and by the Grant of the National Academy of Sciences of Ukraine [grant number 0112U000254.].

ORCID

Galyna P. Volynets http://orcid.org/0000-0002-0166-2642

References

[1] Pan J, Chang Q, Wang X, et al. Reactive oxygen species-activated Akt/ASK1/p38 signaling pathway in nickel compound-induced apoptosis in BEAS 2B cells. Chem Res Toxicol. 2010;23:568–577.
[2] Sano R, Reed JC. ER stress-induced cell death mechanisms. Biochim Biophys Acta. 2013;1833:3460–3470.
[3] Sumbayev V. LPS-induced Toll-like receptor 4 signalling triggers cross-talk of apoptosis signal-regulating kinase 1 (ASK1) and HIF-1alpha protein. FEBS Lett. 2008;582:319–326.
[4] Rastogi S, Rizwani W, Joshi B, et al. TNF-α response of vascular endothelial and vascular smooth muscle cells involve differential utilization of ASK1 kinase and p73. Cell Death Differ. 2012;19:274–283.
[5] Song J, Park KA, Lee WT, et al. Apoptosis signal regulating kinase 1 (ASK1): potential as a therapeutic target for Alzheimer's disease. Int J Mol Sci. 2014;15:2119–2129.
[6] Lee KW, Woo JM, Im JY, et al. Apoptosis signal-regulating kinase 1 modulates the phenotype of α-synuclein transgenic mice. Neurobiol Aging. 2015;36:519–526.
[7] Toyama K, Koibuchi N, Uekawa K, et al. Apoptosis signal-regulating kinase 1 is a novel target molecule for cognitive impairment induced by chronic cerebral hypoperfusion. Arterioscler Thromb Vasc Biol. 2014;34:616–625.
[8] Nakamura T, Kataoka K, Fukuda M, et al. Critical role of apoptosis signal-regulating kinase 1 in aldosterone/salt-induced cardiac inflammation and fibrosis. Hypertension. 2009;54:544–551.
[9] Guo X, Harada C, Namekata K, et al. Regulation of the severity of neuroinflammation and demyelination by TLR-ASK1-p38 pathway. EMBO Mol Med. 2010;2:504–515.
[10] Mnich SJ, Blanner PM, Hu LG, et al. Critical role for apoptosis signal-regulating kinase 1 in the development of inflammatory K/BxN serum-induced arthritis. Int Immunopharmacol. 2010;10:1170–1176.
[11] Yamaguchi K, Takeda K, Kadowaki H, et al. Involvement of ASK1-p38 pathway in the pathogenesis of diabetes triggered by pancreatic β cell exhaustion. Biochim Biophys Acta. 2013;1830:3656–3663.
[12] Iriyama T, Takeda K, Nakamura H, et al. ASK1 and ASK2 differentially regulate the counteracting roles of apoptosis and inflammation in tumorigenesis. EMBO J. 2009;28:843–853.
[13] Hayakawa Y, Hirata Y, Nakagawa H, et al. Apoptosis signal-regulating kinase 1 and cyclin D1 compose a positive feedback loop contributing to tumor growth in gastric cancer. Proc Natl Acad USA. 2011;108:780–785.
[14] Brys R, Gibson K, Poljak T, et al. Chapter three – discovery and development of ASK1 inhibitors. Prog Med Chem. 2020;59:101–179.
[15] Volynets GP, Bdzhola VG, Kukharenko OP, et al. Protein kinase ASK1 as potential therapeutic target. Biopolym Cell. 2009;25:169–180.
[16] Okamoto M, Saito N, Kojima H, et al. Identification of novel ASK1 inhibitors using virtual screening. Bioorg Med Chem. 2011;19:486–489.
[17] Terao Y, Suzuki H, Yoshikawa M, et al. Design and biological evaluation of imidazo[1,2-a]pyridines as novel and potent ASK1 inhibitors. Bioorg Med Chem Lett. 2012;22:7326–7329.
[18] Singh O, Shillings A, Craggs P, et al. Crystal structures of ASK1-inhibitor complexes provide a platform for structure-based drug design. Protein Sci. 2013;22:1071–1077.
[19] Volynets GP, Bdzhola VG, Kukharenko OP, et al. Identification of low-molecular inhibitors of proteinase ASK1. Ukr Biokhim Zh. 2010;82:41–50.
[20] Volynets GP, Chekanov MO, Synyugin AR, et al. Identification of 3H-naphtho[1,2,3-de]quinoline-2,7-diones as inhibitors of apoptosis signal-regulating kinase 1 (ASK1). J Med Chem. 2011;54:2680–2686.
[21] Volynets GP, Bdzhola VG, Golub AG, et al. Rational design of apoptosis signal-regulating kinase 1 inhibitors: discovering novel structural scaffold. Eur J Med Chem. 2013;61:104–115.
[22] Starosyla SA, Volynets GP, Lukashov SS, et al. Identification of apoptosis signal-regulating kinase 1 (ASK1) inhibitors among the derivatives of benzothiazol-2-yl-3-hydroxy-5-phenyl-1,5-dihydropyrrol-2-one. Bioorg Med Chem. 2015;23:2489–2497.
[23] Tesch GH, Ma FY, Han Y, et al. ASK1 inhibitor halts progression of diabetic nephropathy in *Nos3*-deficient mice. Diabetes. 2015;64:3903–3913.
[24] Zheng S, Long L, Li Y, et al. A novel ASK inhibitor AGI-1067 inhibits TLR-4-mediated activation of ASK1 by preventing dissociation of thioredoxin from ASK1. Cardiovasc Pharm Open Access. 2015;4(132).
[25] Wang Y, Hou S, Tong Y, et al. Discovery of potent apoptosis signal-regulating kinase 1 inhibitors via integrated computational strategy and biological evaluation. J Biomol Struct Dyn. 2020;38:4385–4396.
[26] Monastyrskyi A, Bayle S, Quereda V, et al. Discovery of 2-arylquinazoline derivatives as a new class of ASK1 inhibitors. Bioorg Med Chem Lett. 2018;28:400–404.
[27] Lanier M, Pickens J, Bigi SV, et al. Structure-based design of ASK1 inhibitors as potential agents for heart failure. ACS Med Chem Lett. 2017;8:316–320.
[28] Gibson TS, Johnson B, Fanjul A, et al. Structure-based drug design of novel ASK1 inhibitors using an integrated lead optimization strategy. Bioorg Med Chem Lett. 2017;27:1709–1713.
[29] Lovering F, Morgan P, Allais C, et al. Rational approach to highly potent and selective apoptosis signal-regulating kinase 1 (ASK1) inhibitors. Eur J Med Chem. 2018;145:606–621.
[30] Himmelbauer MK, Xin Z, Jones JH, et al. Rational design and optimization of a novel class of macrocyclic apoptosis signal-regulating kinase 1 inhibitors. J Med Chem. 2019;62:10740–10756.
[31] Xin Z, Himmelbauer MK, Jones JH, et al. Discovery of CNS-penetrant apoptosis signal-regulating kinase 1 (ASK1) inhibitors. ACS Med Chem Lett. 2020;11:485–490.
[32] Zhang S, Huang C, Lyu X, et al. Discovery of a 2-pyridinyl urea-containing compound YD57 as a potent inhibitor of apoptosis signal-regulating kinase 1 (ASK1). Eur J Med Chem. 2020;195:112277.
[33] Doudou S, Sharma R, Henchman RH, et al. Inhibitors of PIM-1 kinase: a computational analysis of the binding free energies of a range of imidazo[1,2-b]pyridazines. J Chem Inf Model. 2010;50:368–379.
[34] Lan NT, Vu KB, Ngoc MKD, et al. Prediction of AChE-ligand affinity using the umbrella sampling simulation. J Mol Graph Model. 2019;93:107441.
[35] Ngo ST, Vu KB, Bui LM, et al. Effective estimation of ligand-binding affinity using biased sampling method. ACS Omega. 2019;4:3887–3893.
[36] Wu C, Chen X, Chen D, et al. Insight into ponatinib resistance mechanisms in rhabdomyosarcoma caused by the mutations in FGFR4 tyrosine kinase using molecular modeling strategies. Int J Biol Macromol. 2019;135:294–302.
[37] Zhang Z, Xu Y, Wu J, et al. Exploration of the selective binding mechanism of protein kinase aurora A selectivity via a comprehensive molecular modeling study. PeerJ. 2019;7:e7832.
[38] Bamborough P, Brown M, Christopher J, et al. Selectivity of kinase inhibitor fragments. J Med Chem. 2011;54:5131–5143.

[39] Berendsen HJC, van der Spoel D, van Brunen R. GROMACS: A message-passing parallel molecular dynamics implementation. Comp Phys Comm. 1995;91:43–56.
[40] van der Spoel D, Lindahl E, Hess B, et al. GROMACS: fast, flexible and free. J Comput Chem. 2005;26:1701–1718.
[41] Hess B, Kutzner C, van de Spoel D, et al. GROMACS 4: algorithms for highly efficient, load-balanced, and scalable molecular simulation. J Chem Theory Comput. 2008;4:435–447.
[42] Oostenbrink C, Villa A, Mark AE, et al. A biomolecular force field based on the free enthalpy of hydration and solvation: The GROMOS force-field parameter sets 53A5 and 53A6: the GROMOS force-field parameter sets 53A5 and 53A6. J Comput Chem. 2004;25:1656–1676.
[43] Hockney RW, Goel SP, Eastwood J. Quiet high resolution computer models of a plasma. J Comput Phys. 1974;14:148–158.
[44] Darden T, York D, Pedersen L. Particle mesh Ewald: an N log(N) method for Ewald sums in large systems. J Chem Phys. 1993;98:10089–10092.
[45] Essmann U, Perera L, Berkowitz ML, et al. A smooth particle mesh Ewald method. J Chem Phys. 1995;103:8577–8593.
[46] Hub JS, de Groot BL, van der Spoel D. G_wham – a free weighted histogram analysis implementation including robust error and autocorrelation estimates. J Chem Theory Comput. 2010;6:3713–3720.
[47] Schüttelkopf AW, van Aalten MF. PRODRG: a tool for high-throughput crystallography of protein-ligand complexes. Acta Cryst. 2004;D60:1355–1363.
[48] Berendsen HJC, Postma JPM, van Gunsteren WF, et al. Interaction models for water in relation to protein hydration. In: B Pullman, editor. Intermolecular forces. Boston (MA): D. Reidel Publishing Company; 1981. p. 331–342.
[49] Bjelkmar P, Larsson P, Cuendet MA, et al. Implementation of the CHARMM force field in GROMACS: analysis of protein stability effects from correction maps, virtual interaction sites, and water models. J Chem Theory Comput. 2010;6:459–466.
[50] Jorgensen WL, Chandrasekhar J, Madura JD. Comparison of simple potential functions for simulating liquid water. J Chem Phys. 1983;79:926–935.
[51] Lemkul JA, Bevan DR. Assessing the stability of Alzheimer's amyloid protofibrils using molecular dynamics. J Phys Chem B. 2010;114:1652–1660.